Characterization and Modelization of the Geometrical and Flow Properties of Fractured Carbonates: Application to Amellago Outcrop Data*

I. Malinouskaya[1], P. M. Adler[1], J.-F.Thovert[2], and V. Mourzenko[2]

Search and Discovery Article #120075 (2012)*
Posted December 31, 2012

*Adapted from extended abstract prepared in conjunction with poster presentation at AAPG Hedberg Conference, Fundamental Controls on Flow in Carbonates, July 8-13, 2012, Saint-Cyr Sur Mer, Provence, France, AAPG©2012

[1]UPMC Sisyphe, Paris, France (malinoui@gmail.com)
[2]Institut PPRIME, Futuroscope, France

Abstract

Fractures influence the hydraulic and transport properties of the natural geological formations. The purpose of the present work is to predict the properties of the fractured carbonates, in particular, the percolation status and permeability.

These properties can be obtained either using theoretical predictions for some standard cases or applying direct numerical simulations. Both approaches are based on statistical geometrical characteristics of the fracture networks. In the first case, existing models are directly applied. In the second case, the hydraulic properties are obtained by solving the governing flow equations, which are written on the local scale and applied to the fracture network, represented in an explicit way. Since a real fully described 3D sample cannot be provided, reconstructed ones are obtained based on the statistical geometrical characteristics of the real networks. Therefore, these characteristics are essential for the prediction of the hydraulic properties whatever the method.

The statistical geometrical characteristics are not always available in explicit form. In order to determine them, some measurements of the field data are required. There are several stereological methods, which can be used to determine the required parameters from the available field measurements (Berkowitz and Adler, 1998; Gupta and Adler, 2006; Thovert and Adler, 2005; Mourzenko et. al., 2011a).

Introduction

We study data collected from several windows in the Amellago outcrop. These data include field measurements of the fracture orientations and trace maps drawn from photographs, represented by coordinates of trace end points. Field measurements on a horizontal pavement are also provided. They consist in a list of trace lengths, of the corresponding azimuths and of the nature of the trace terminations (inside or outside of the observation domain).

The hydraulic properties are obtained as follows. The observations from several windows in the Amellago outcrop and the corresponding trace maps are studied. The treatment and subsequent analysis of the available field data allow determining or calibrating the model parameters. Then, the permeability tensor is derived using existing theoretical models for generic cases. These estimations are easy in terms of computations, but they do not include any specific features and therefore they can only provide a priori and possibly rough approximations. Finally, full numerical simulations are performed.

Geometrical Characteristics

A 3D network of plane, possibly polydisperse fractures of the identical shapes is characterized by the mean fracture area $\langle A \rangle$, the mean fracture perimeter $\langle P \rangle$, the density ρ which is defined as the number of fractures per unit volume, and the shape factor η_p=4R/P where R is the radius of the disk circumscribed to a fracture. The dimensionless density ρ' is defined as the average number of intersections per fracture. The normals to the fracture **n** can be distributed isotropically or according to a Fisher distribution with a pole given by its polar coordinates (θ_0,ψ_0) and with a parameter κ, or directly provided by a set of field observations.

If the fractures are isotropically oriented within their plane, some geometrical characteristics can be related to measured 2D parameters. For instance, assuming that there is no correlation between fracture size and orientation, the average number of trace per unit area Σ_t, the trace length per unit area $\mathcal{C}$ and the average trace length $\langle c \rangle$ are given by (Mourzenko, et. al., 2011a).

$$\Sigma_t = \rho \langle P \rangle \frac{\langle \sin \alpha \rangle}{\pi}, \quad \mathcal{C} = \rho \langle A \rangle \langle \sin \alpha \rangle, \quad \langle c \rangle = \pi \frac{\langle A \rangle}{\langle P \rangle} \tag{1}$$

where α is an angle between the normal to observation plane and the normal to the fracture.

Model Parameters

In order to describe a 3D fracture network, the fracture positions, orientations and shapes, the fracture size distribution and the network density are required. In order to simplify the model, a few hypotheses are used. First, we suppose that the fracture positions are random, without spatial correlation. This assumption is supported by the analysis of the variograms of spacings between successive intersections along scanlines, which does not reveal any spatial correlations.

Second, the fractures are regarded as rectangles, with their longer side oriented horizontally; *a* and *b(a)* are the shorter and longer sides of the fracture, respectively, and *f* is the constant aspect ratio, *b(a)=fa*. The correlation coefficient for the trace lengths and orientations is very small; therefore, we assume that there is no correlation between fracture size and orientation. The size distribution is described by the number-pdf *n(a)*.

Finally, the density ρ is supposed to be uniform over the investigated domain.

Consider the data provided for one of the vertical observation windows in Amellago outcrop. The trace maps are studied first (Figure 1). Within the sampling domain Ω, the trace length per unit area is calculated as $\mathcal{C} = \sum_{\Omega} c / |\Omega| = 1.56$ m^{-1} and the number of traces per unit area as $\Sigma_t = \sum_{\Omega} N_t / |\Omega| = 1.51$ m^{-2}; thus, their ratio yields the mean trace length $\langle c \rangle_{\Omega}$=1.04 m. Similarly, for the horizontal pavement, one obtain $\langle c \rangle_{p}$=4.09 m.

The analysis of the trace length distribution in the vertical window allows to determine the corresponding number-pdf $\varphi(c) = \frac{1}{\lambda} \exp\left\{-\frac{c-c_0}{\lambda}\right\}$ with λ=0.74 m and c_0=0.2 m.

The field measurements of the 3D fracture orientations are directly used in the numerical simulations. The parameter $\langle \sin \alpha \rangle$ in Berkowitz and Adler (1998) is found to be equal to 0.83. On the other hand, a modelization by a Fisher distribution is possible, with a pole pointing at ψ_0=N117° and θ_0=79° from the vertical, and a concentration parameter κ=6.1.

Then, the relations between measured 2D parameters and 3D geometrical characteristics are established. The aspect ratio f is derived by a comparison of the trace lengths in the vertical window and in the horizontal pavement. The volumetric density $\rho\langle A \rangle$ results from $\mathcal{C}$ and from the fracture orientations $\langle \sin \alpha \rangle$. Then, the network density ρ is obtained from Σ_t and the number-pdf for the fracture size distribution is found by $n(a) = \varphi(a)\langle a \rangle / a$. Thus, the mean fracture size $\langle a \rangle$ is determined as the harmonic average of the trace lengths $\langle c^{-1} \rangle^{-1}$. The model parameters are summarized by

$$f = 3.95, \quad \langle a \rangle = 0.57 \text{ m}, \quad \rho\langle A \rangle = 1.89 \text{ m}^{-1} \quad \rho = 0.82 \text{ m}^{-3}, \quad n(a) = \frac{1}{1.31a} \exp\left\{-\frac{a-0.2}{0.74}\right\} \text{m}^{-1} \tag{2}$$

Permeability Prediction

The permeability **K** results from the flow problem governed by a two-dimensional Darcy law in the fractures and the mass conservation equations. **K** is defined as the coefficient, which relates the resulting macroscopic flux to the imposed macroscopic pressure gradient.

A number of theoretical models exist to predict the permeability in various generic cases, which are summarized in (Mourzenko et. al, 2011b). In particular, the Snow model (Snow, 1969) is used for very well connected fracture networks, *i.e.* when ρ' is very large

$$\mathbf{K}_s = K_{si}\mathbf{\Psi}, \quad K_{si} = \frac{2}{3}\rho\langle A \rangle \sigma, \quad \mathbf{\Psi} = \frac{3}{2}\langle \mathbf{I} - \mathbf{nn} \rangle \tag{3}$$

where K_{si} is the permeability for an isotropic fracture distribution, σ is the fracture permeability, which is taken uniform within each fracture and constant for all the fractures. $\mathbf{\Psi}$ incorporates the effect of the geometrical anisotropy.

The geometrical tensor $\mathbf{\Psi}$ is directly obtained from the 3D orientation field data. On the other hand, it can be calculated supposing that the fractures are oriented according to a Fisher distribution. Both methods yield nearly the same results.

General results also exist for finite fracture networks with smaller densities, which take into account the degree of connectivity of the network (Mourzenko et. al, 2011b). Assuming that the fractures are isotropically randomly oriented within their plane, a very good estimate of the network permeability is provided by

$$\mathbf{K} = K_{si}\tilde{K}\mathbf{\Psi} \tag{4}$$

where $\tilde{K}$ only depends on the dimensionless density ρ' which quantifies the network connectivity.

If the fractures are monodisperse rectangles, isotropically oriented within their plane, with the values of f, ρ, and $\rho\langle A\rangle$ in Gupta and Adler (2006), $\tilde{K}$ is equal to 0.18.

These estimations provide only rough approximations. Therefore, full numerical simulations are performed. The results are compared with the theoretical models to show if specific features of the present formation strongly influence its hydraulic properties or not.

For the numerical simulations, the fractures are generated in a cell periodic along the x and y-axes and non-periodic along z-axis (Huseby et. al., 1997). The fracture orientations are taken directly from the list of the 3D measured data. The centers obey a Poisson distribution. The fractures are horizontal rectangles with the constant aspect ratio f. In order to solve the flow problem, the fracture network is discretized by triangulation (Koudina et. al., 1998). The resulting triangular mesh explicitly contains the fracture intersections. Then, the reconstructed networks are used to calculate the permeability tensor (Mourzenko et. al, 2011b).

A set of 10 polydisperse fracture networks has been reconstructed (Figure 2) using the model parameters (Gupta and Adler, 2006). The resulting permeability tensor is calculated for each sample and the mean over all the samples is taken. It is compared with the theoretical models (Huseby et. al., 1997; Koudina et. al, 1998). The permeability $\tilde{K}$, relative to the expected value K_{si} for isotropic networks with the same volumetric area is equal to 0.32, which is larger than the corresponding result of the generic model (Koudina et. al., 1998). However, the anisotropy of the network permeability complies accurately with the anisotropy of the geometric tensor $\mathbf{\Psi}$ in the horizontal plane.

In order to test the influence of the fracture size polydispersity, the simulations have been conducted with the monodisperse networks according to different rules. First, the fracture size is equal to $\langle a\rangle$ (Gupta and Adler, 2006), *i.e.*, the density Σ_t is conserved but $\mathcal{C}$ is underestimated. Second, the fracture size is set to $\langle a^2\rangle^{1/2}$, *i.e.*, $\mathcal{C}$ and $\rho\langle A\rangle$ are conserved. Finally, a third set of calculations was conducted with a fracture size equal to $\langle a^3\rangle^{1/3}$; $\rho\langle A\rangle$ is overestimated, but ρ' is preserved.

Again, all the results have the same anisotropy as $\mathbf{\Psi}$ in the horizontal plane. However, $\tilde{K}$ is very different for each case. In the first case, $\tilde{K}_1 = 0.0033$ is much smaller than $\tilde{K} = 0.32$ obtained for polydisperse networks and only 50% of the samples are found percolating. The permeability $\tilde{K}_2 = 0.22$ in the second case is close to prediction (Koudina et. al., 1998) for 4-rectangles, but smaller than the polydisperse one. In the third case, $\tilde{K}_3 = 0.62$ exceeds the result of $\tilde{K}_1$ since the network connectivity is preserved while volumetric area is overestimated.

Conclusions

The methods, which are applied to obtain the geometrical characteristics of the fracture networks using the available field observations, are presented. The model parameters are determined and used for the theoretical predictions and for the direct numerical simulations.

The influence of the various parameters on the network properties can be examined by modifying values of the model parameters (Gupta and Adler, 2006) or of the measured quantities in (Berkowitz and Adler, 1998). This can provide indications about the sensibility of the predictions on the field data, about which ones should be determined with special care and which ones could be estimated in a more approximate way, and possibly guidelines for data acquisition.

References

Berkowitz, B., and P.M. Adler, 1998, Stereological analysis of fracture network structure in geological formations: Journal Geophysical Research, v. 103/B7, p. 15,339-15,360.

Gupta, A.K., and P.M. Adler, 2006, Stereological analysis of fracture networks along cylindrical galleries: Mathematical Geology, v. 38/3, p. 233-267.

Huseby, O., J.-F. Thovert, and P.M. Adler, 1997, Geometry and topology of fracture systems: Journal of Physics A, v. 30, p. 1415-1444.

Koudina, N., R. Gonzalez Garcia, J.-F. Thovert, and P.M. Adler, 1998, Permeability of three-dimensional fracture networks: Physical Review E, v. 57/4, p. 4466-4479.

Mourzenko, V.V., J.-F. Thovert, and P.M. Adler, 2011, Trace analysis for fracture networks with anisotropic orientations and heterogeneous distributions: Physical Review E, v. 83/3, 18 p.

Mourzenko, V.V., J.-F. Thovert, and P.M. Adler, 2011, Permeability of isotropic and anisotropic fracture networks, from the percolation threshold to very large densities: Physical Review E, v. 84/3, 20 p.

Snow, D.T., 1969, Anisotropie Permeability of Fractured Media: Water Resources Research, v. 5/6, p. 1273-1289.

Thovert, J.-F. and P.M. Adler, 2004, Trace analysis for fracture networks of any convex shape: Geophysical Research Letters, v. 31/L22502, 5 p.

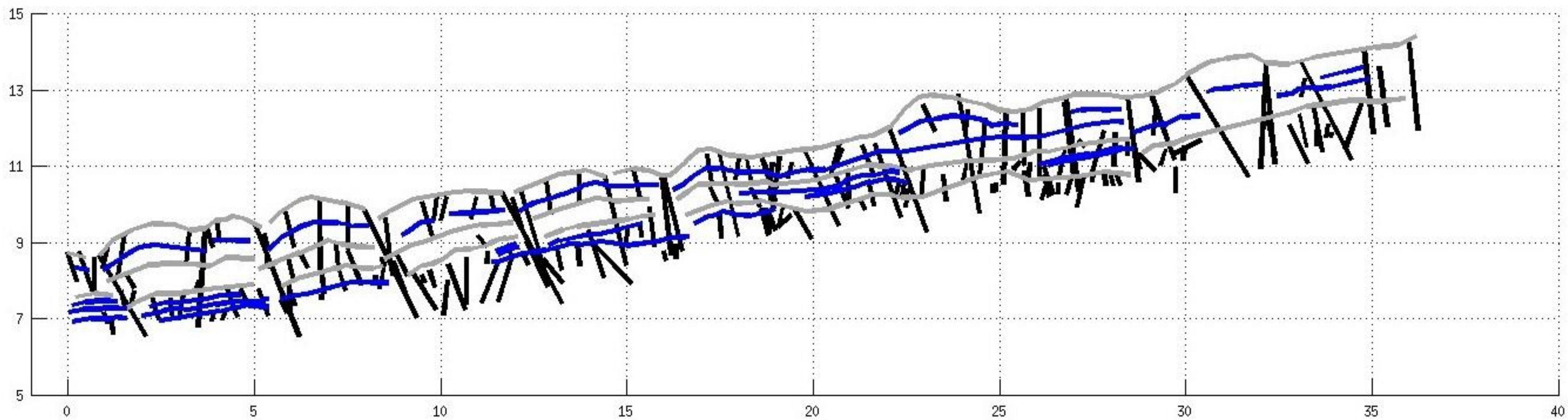

Figure 1. Example of a full end-to-end trace map; the data are for the traces (black), beddings (grey) and stylolites (blue).

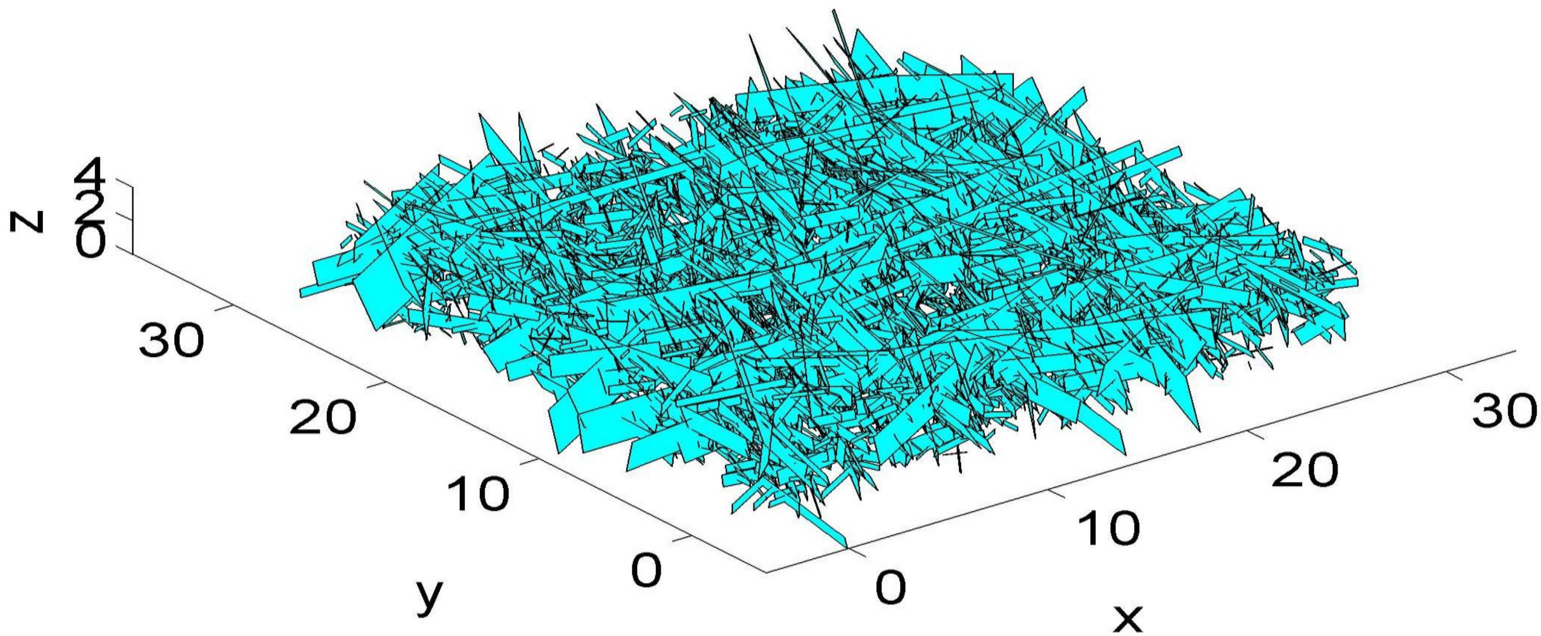

Figure 2. Example of a 3D reconstructed fracture network.